Transient Analysis of Cage Induction Machines Under Stator, Rotor Bar and End Ring Faults

Hamid A. Toliyat
Member IEEE
Texas A&M University
College Station, TX 77843
Fax: (409) 845-6259

Thomas A. Lipo
Fellow IEEE
University of Wisconsin-Madison
Madison, WI 53706
Fax: (608) 262-1267

* On scientific leave from Ferdowsi University-Mashhad, Iran

Keywords: Winding Functions, Stator Failure, Broken Rotor Bars and End-Rings, Induction Machines, Simulation

Abstract - An analysis method is developed for modeling of multi phase cage induction motors with asymmetry in the stator, arising due to an interturn fault resulting in a disconnection of one or more coils making up a portion of a stator phase winding and any distribution and number of rotor bar and end-ring failures. The approach, based on the winding functions, makes no assumption as to the necessity for sinusoidal MMF and therefore include all the space harmonics in the machine. Simulation and experimental results confirm the validity of the proposed method.

I. INTRODUCTION

The induction machine can operate under asymmetrical stator and/or rotor winding connections during such conditions as:

- interturn fault resulting in the opening or shorting of one or more circuits of a stator phase winding.
- abnormal connection of the stator windings.
- broken rotor bar or end-ring.

Asymmetrical operation of induction machines result in unbalanced air gap voltages, consequently unbalanced line currents, increased losses, increased torque pulsations, and decreased average torque [1-5, 7-8, 13]. Consequently, asymmetrical operation of induction machine results in poor efficiency and excessive heating, which eventually leads to the failure of the machine. Therefore, characterization and accurate prediction of the degradation of the performance of the induction machine under such conditions is of considerable importance.

94 SM 361-6 EC A paper recommended and approved by the IEEE Electric Machinery Committee of the IEEE Power Engineering Society for presentation at the IEEE/PES 1994 Summer Meeting, San Francisco, CA, July 24 - 28, 1994. Manuscript submitted October 4, 1993; made available for printing June 1, 1994.

The transient analysis of the induction machine with asymmetrical rotor cage is also important for on line monitoring of large motors. The problem of effectively modeling the asymmetries in the stator and rotor with the concomitant effects of space harmonics is of increasing importance for studying the degradation of the performance of induction motor drive systems and for on line monitoring of large motors. With the increased use of inverter supplied induction motors for adjustable speed drives (ASDs) systems, characterization and accurate prediction of the degradation of the transient performance of the motor drive system arising due to the asymmetrical stator and/or rotor winding connections, has become of significant importance. This is because of the necessity of accurate determination of the additional derating required of the motor, due to the adverse effects of non sinusoidal impressed voltages.

The existence of space harmonics is well known to have a significant detrimental effect on the steady state and transient characteristics of the machine, such as significant torque pulsations which may cause cogging and crawling. Since the existing approaches lack the ability to predict the derating of the machine required due to the adverse effects of the space harmonics, the Winding Function Approach (WFA) is used which accounts for all the space harmonics in the machine.

The transient analysis of the induction machine for the case of rotor asymmetry, resulting due to either a broken rotor bar or broken end-ring, has in general received less attention than the case of stator asymmetry due to the complexity of modeling. Weichel and Mishkin [1,2], discuss the case of rotor asymmetry arising due to the broken end-ring for a squirrel cage induction machine. Steady state analysis of the induction machine for the case of rotor asymmetry, due to broken rotor bars has already been reported in [3-5], based on the method of symmetrical component theory and in [6], using dqn theory. As already mentioned, this analysis is based on the assumption of the absence of higher order space harmonics in the machine and can not accurately predict the transient characteristics of the machine. Thus, to the authors' knowledge tools for the transient analysis of the induction machine for the case of rotor asymmetry, due to a broken rotor bar and/or end-ring are not available. A computer based instrument for detection of broken rotor bars and open end rings in squirrel cage

0885-8969/95/$04.00 © 1994 IEEE

induction motors has been reported in [7]. The adverse effects of broken rotor bars in squirrel cage induction motors are excessive vibration, noise and sparking during starting. These effects become noticeable when the fault in the rotor has substantially grown to involve several broken bars, making the detection of one broken rotor bar in the machine, as mentioned in [7] a very difficult task.

In a previous paper [8] a study of multiphase induction machines under phase impedance unbalance conditions was given. In this paper a comprehensive analysis of multiphase cage induction machines under stator or rotor asymmetries is presented.

II. Modeling Induction Machines with m Stator Phases and n Rotor Bars

In [9-10] the differential equations predicting the performance of an m phase induction machine with n rotor bars were derived. This model is based on coupled magnetic approach by considering that the current in each bar is an independent variable. The effects of non-sinusoidal air-gap MMF produced by both the stator and the rotor currents have been incorporated into the model. This approach has been successfully applied to predict the performance of induction and synchronous reluctance machines [11-12], with multiple phases and general winding connections such as concentrated, concentric and multiple layer with different pitch factor, including space and time harmonics.

Consider initially a general m-n winding machine with the following assumptions,

-negligible saturation
-uniform air-gap
-m identical stator windings with axes of symmetry
-n uniformly distributed cage bars or identical rotor windings with axes of symmetry such that even harmonics of the resulting spatial winding distribution are zero
-eddy current, friction, and windage losses are neglected
-insulated rotor bars

The cage rotor can be viewed as n identical and equally spaced rotor loops. For example, the first loop may consist of the 1st and (k+1)th rotor bars and the connecting portions of the end rings between them, where k is any arbitrarily chosen integer ($1 \le k \le n$) and the second loop consists of the 2nd and (k+2)th rotor bar and the connecting portions of the end rings between them and so on. For a cage having n bars, there are 2n nodes and 3n branches. Therefore, the current distribution can be specified in terms of n+1 independent rotor currents. These currents comprise of the n rotor loop currents (i_k^r)plus a circulating current in one of the end rings (i_e). Obviously, in a motor with complete end rings, (i_e) would be equal zero. The n rotor loop currents are coupled to each other and to the stator winding, through the mutual inductances. However, the end ring loop current does not couple with the stator windings, and couples with the rotor loops currents only through the end ring leakage inductance and the end ring resistance.

Stator Voltage Equations

The voltage equations for the stator loops can be written as,

$$V_s = R_s I_s + \frac{d\Lambda_s}{dt} \tag{1}$$

where

$$\Lambda_s = L_{ss} I_s + L_{sr} I_r \tag{2}$$

and

$$I_s = \left(i_1^s \; i_2^s \; \ldots\ldots\ldots \; i_m^s \right) \tag{3}$$

$$I_r = \left(i_1^r \; i_2^r \; \ldots\ldots\ldots\ldots \; i_n^r \; i_e \right) \tag{4}$$

$$V_s = \left(v_1^s \; v_2^s \; \ldots\ldots\ldots \; v_m^s \right) \tag{5}$$

The matrix R_s is a diagonal m by m consists of resistances of each coil. Due to conservation of energy, the matrix L_{ss} is a symmetric m by m matrix. The mutual inductance matrix L_{sr} is an m by n matrix comprised of the mutual inductances between the stator coils and the rotor loops.

$$L_{sr} = \begin{pmatrix} L_{11}^{sr} & L_{12}^{sr} & \ldots\ldots\ldots\ldots & L_{1n}^{sr} & L_{1e}^{sr} \\ L_{21}^{sr} & L_{22}^{sr} & \ldots\ldots\ldots\ldots & L_{2n}^{sr} & L_{2e}^{sr} \\ \vdots & \vdots & \ldots\ldots\ldots\ldots & \vdots & \vdots \\ L_{m1}^{sr} & L_{m2}^{s} & \ldots\ldots\ldots\ldots & L_{mn}^{sr} & L_{me}^{sr} \end{pmatrix} \tag{6}$$

The second term of equation (1) can typically be written in the form,

$$\frac{d\Lambda_s}{dt} = L_{ss} \frac{dI_s}{dt} + \omega_{rm} \frac{dL_{sr}}{d\theta_{rm}} I_r + L_{sr} \frac{dI_r}{dt} \tag{7}$$

where, θ_{rm} is the spatial position of the rotor and rotor mechanical speed is,

$$\omega_{rm} = \frac{d\theta_{rm}}{dt} \tag{8}$$

Rotor Voltage Equations

The representation of an induction machine with a cage rotor is fundamentally the same as one with a phase wound rotor where it is assumed that the cage rotor can be replaced by a set of mutually coupled loops. One particular advantage of this approach is that it is also applicable to cage rotors with non-integral numbers of rotor bars per pole pair. From Figure 1 the voltage equations for the rotor loops are

$$V_r = R_r I_r + \frac{d\Lambda_r}{dt} \tag{9}$$

where,

$$V_r = \left(v_1^r \; v_2^r \; \ldots\ldots\ldots\ldots \; v_n^r \; v_e \right)$$

In case of a cage rotor the rotor end ring voltage, v_e=0, and rotor loop voltages, v_k^r= 0 ; k = 1, 2 ... n. The rotor flux linkages Λ_r can be written as,

$$\Lambda_r = L_{sr}^t I_s + L_{rr} I_r \tag{10}$$

where the matrix L_{sr}^t is the transpose of the matrix L_{sr} and the matrix L_{rr} is the n+1 by n+1 symmetric matrix. The matrix R_r is n+1 by n+1 symmetric where, R_e is the end ring segment resistance, and R_b is the rotor bar resistance.

$$R_r = \begin{bmatrix} 2(R_b+R_e) & -R_b & 0 & \cdots & 0 & -R_b & -R_e \\ -R_b & 2(R_b+R_e) & -R_b & \cdots & 0 & 0 & -R_e \\ \vdots & \vdots & \vdots & \vdots & \vdots & \vdots & \vdots \\ \vdots & \vdots & \vdots & \vdots & \vdots & \vdots & \vdots \\ 0 & 0 & 0 & \cdots & 2(R_b+R_e) & -R_b & -R_e \\ -R_b & 0 & 0 & \cdots & -R_b & 2(R_b+R_e) & -R_e \\ -R_e & -R_e & -R_e & \cdots & -R_e & -R_e & nR_e \end{bmatrix} \tag{11}$$

In equation (12), L_{mr} is the magnetizing inductance of each rotor loop, L_b the rotor bar leakage inductance, L_e the rotor end ring leakage inductance, and $L_{r_i r_k}$ the mutual inductance between two rotor loops.

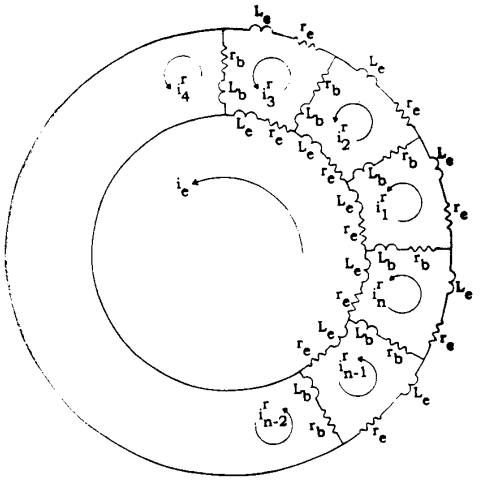

Figure 1 Equivalent circuit of squirrel cage rotor showing rotor loop currents and circulating end ring current.

$$L_{rr} = \begin{bmatrix} L_{mr}+2(L_b+L_e) & L_{r_1r_2}-L_b & L_{r_1r_3} & \cdots & L_{r_1r_{n-1}} & L_{r_1r_n}-L_b & -L_e \\ L_{r_2r_1}-L_b & L_{mr}+2(L_b+L_e) & L_{r_2r_3}-L_b & \cdots & L_{r_2r_{n-1}} & L_{r_2r_n} & -L_e \\ \vdots & \vdots & \vdots & \cdots & \vdots & \vdots & \vdots \\ \vdots & \vdots & \vdots & \cdots & \vdots & \vdots & \vdots \\ L_{r_{n-1}r_1} & L_{r_{n-1}r_2} & L_{r_{n-1}r_3} & \cdots & L_{mr}+2(L_b+L_e) & L_{r_{n-1}r_n} & -L_e \\ L_{r_nr_1}-L_b & L_{r_nr_2} & L_{r_nr_3} & \cdots & L_{r_nr_{n-1}} & L_{mr}+2(L_b+L_e) & -L_e \\ -L_e & -L_e & -L_e & \cdots & -L_e & -L_e & nL_e \end{bmatrix} \tag{12}$$

Calculation of Torque

The mechanical equation of motion depends upon the characteristics of the load which may differ widely from one application to the next. We will assume here, for simplicity, that the torque which opposes that produced by the machine consists only of an inertial torque and an external load torque which are known explicitly. In this case the mechanical equation of motion is simply,

$$J\frac{d^2\theta_{rm}}{dt^2} + T_L = T_e \tag{13}$$

where T_L is the load torque, and T_e is the electromagnetic torque produced by the machine. The electrical torque can be found from the magnetic coenergy W_{co} as,

$$T_e = \left(\frac{\delta W_{co}}{\delta \theta_{rm}}\right)_{(I_s,\ I_r \text{constant})} \tag{14}$$

In a linear magnetic system the coenergy is equal to the stored magnetic energy so that,

$$W_{co} = \frac{1}{2} I_s^t L_{ss} I_s + \frac{1}{2} I_s^t L_{sr} I_r + \frac{1}{2} I_r^t L_{sr}^t I_s + \frac{1}{2} I_r^t L_{rr} I_r \tag{15}$$

It is obvious that L_{ss} and L_{rr} contain only constant elements and T_e is a scalar quantity. Therefore, after some matrix algebra, the torque equation reduces to the final form

$$T_e = \frac{P}{2} I_s^t \frac{\delta L_{sr}}{\delta \theta_r} I_r \tag{16}$$

where P denote the number of motor poles and θ_r is the rotor displacement in electrical radians.

Calculation of Inductances for the Induction Machine with One of the Two Coils in One Phase Disconnected

All of the relevant inductances for the induction machine can be calculated using the winding function method given in [9]. The specific machine studied in this section to verify the theory is a three phase, 1 hp, 60 Hz, 4 pole, 208/460 V induction machine. The machine has 36 stator slots and 44 rotor bars. This machine has two coils per phase and the stator winding asymmetry is caused due to the disconnection of one of the coils in phase c.

Figure 2 shows the turn function or the MMF distribution of the stator phases for the case of the balanced machine and for the case of stator winding asymmetry in phase c. Table 1 gives the mutual inductances between the "healthy" phase a of the stator and rotor bar 1. Note that the mutual inductance between the phase b and rotor bar 1 is the same as given in Table 1 but shifted to the right by 6γ where γ is the angle between two stator slots in radians. Mutual inductance between phase a and rotor loop 2 is the same as given in Table 1, but shifted to the left by α where α is the angle between two rotor slots. Figure 3 shows the variation of

the mutual inductance of the stator phase with rotor loop, with respect to the rotor position.

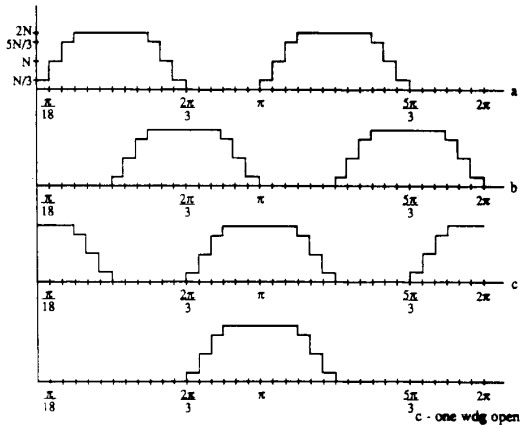

Figure 2 *Turn functions of stator phases. a) All phases "healthy", b) One coil in phase c open.*

$\frac{\mu_0 r\ell N}{g}\left(-\frac{1}{2}\alpha\right)$	$0 \le \theta < \frac{\pi}{18} - \alpha$
$\frac{\mu_0 r\ell N}{g}\left(\theta + \frac{1}{2}\alpha - \frac{\pi}{18}\right)$	$\frac{\pi}{18} - \alpha \le \theta < \frac{\pi}{18}$
$\frac{\mu_0 r\ell N}{g}\left(\frac{1}{2}\alpha\right)$	$\frac{\pi}{18} \le \theta < \frac{2\pi}{18} - \alpha$
$\frac{\mu_0 r\ell N}{g}\left(\theta + \frac{3}{2}\alpha - \frac{\pi}{9}\right)$	$\frac{2\pi}{18} - \alpha \le \theta < \frac{2\pi}{18}$
$\frac{\mu_0 r\ell N}{g}\left(\frac{3}{2}\alpha\right)$	$\frac{2\pi}{18} \le \theta < \frac{\pi}{2} - \alpha$
$\frac{\mu_0 r\ell N}{g}\left(-\theta + \frac{1}{2}\alpha + \frac{\pi}{2}\right)$	$\frac{\pi}{2} - \alpha \le \theta < \frac{\pi}{2}$
$\frac{\mu_0 r\ell N}{g}\left(\frac{1}{2}\alpha\right)$	$\frac{\pi}{2} \le \theta < \frac{5\pi}{9} - \alpha$
$\frac{\mu_0 r\ell N}{g}\left(-\theta - \frac{1}{2}\alpha + \frac{5\pi}{9}\right)$	$\frac{5\pi}{9} - \alpha \le \theta < \frac{5\pi}{9}$
$\frac{\mu_0 r\ell N}{g}\left(-\frac{1}{2}\alpha\right)$	$\frac{5\pi}{9} \le \theta < \frac{11\pi}{18} - \alpha$
$\frac{\mu_0 r\ell N}{g}\left(-\theta - \frac{3}{2}\alpha + \frac{11\pi}{18}\right)$	$\frac{11\pi}{18} - \alpha \le \theta < \frac{11\pi}{18}$
$\frac{\mu_0 r\ell N}{g}\left(-\frac{3}{2}\alpha\right)$	$\frac{11\pi}{18} \le \theta < \pi - \alpha$
$\frac{\mu_0 r\ell N}{g}\left(\theta - \frac{1}{2}\alpha - \pi\right)$	$\pi - \alpha \le \theta < \pi$

Table 1 *Mutual inductance between the "healthy" phase a of the stator and rotor loop 1.*

Calculation of Inductances for the Induction Machine with Rotor Bar and End-Ring Faults

The machine analyzed in this section is a three phase, 7.5 hp, 60 Hz, 4 pole, 460 V induction machine. The machine has 36 stator slots and 28 rotor bars with two coils per stator phase. Figure 4(a) displays the turns function for rotor loop 28 and Figure 4(b) illustrates the turn function for rotor loop 27 for the case that bar number 28 is broken.

As can be seen from the turns function diagrams, the detailed modeling of the machine has been done considering each stator slots and each rotor bar and rotor loop, and no approximations such as the windings being concentrated under a pole face are done. For the specified applied stator voltages, the currents in each rotor loop, stator phase currents, stator and rotor fluxes, torque and speed are computed.

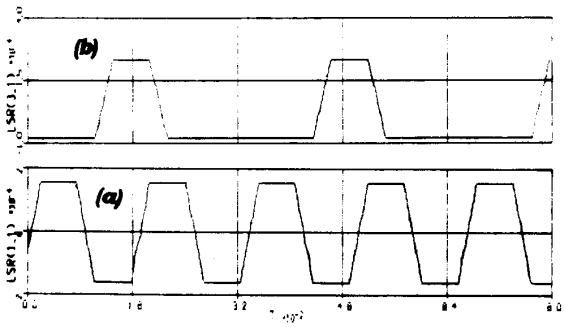

Figure 3 *(a) Mutual inductance between "healthy" phase a of the stator and rotor loop 1. (b) Mutual inductance between the shorted phase c of the stator and rotor loop 1.*

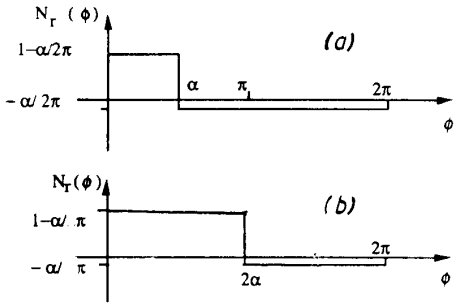

Figure 4 *a) Turn function for rotor loop 28, "healthy". b)Turn function for rotor loop 27, "broken bar #28".*

III. Simulation Results

The specification of the induction machines simulated are as given in the appendix. Simulation of the stator winding asymmetry due to the disconnection of one of the two coils of the phase c, and for the rotor asymmetry due to a broken rotor bar, are given for both the balanced sinusoidal voltage supply (208 V rms) and six-step voltage source inverter supply (vdc=269.7 V). A no load operation has been assumed for all the cases. Figure 5 shows the instantaneous electromagnetic torque, speed and the phase currents of the machine during a start up for the case of the balanced sinusoidal voltage supply and stator windings. Figure 6 illustrates the asymmetrical operation of induction machine. An increased current in the phase c of the machine during transient and steady state conditions is obvious. This rise was noted to be approximately 40% compared to the symmetrically balanced case.

Rotor faults have been simulated by including proper relationships between the rotor current variables, and reducing the coupling inductance matrix. If the bar between loop n-1 and loop n is open circuited, then we require $i^r_{n-1} = i^r_n$ which means that the current i^r_{n-1} is flowing in a double width loop as shown in Figure 7(a). This condition is impressed on the inductance matrix L_{rr} by adding the column relating to i^r_{n-1}, meaning the column n-1 to that relating to i^r_n which is the column n. The same relationship is applied to the corresponding rows. Similar measures are taken for the resistance matrix R_r. The same is done on the column of mutual inductance matrix L_{sr}. Further open circuited bars are incorporated by repeating the above mentioned reduction process, as required. For a broken end ring in the section of the nth rotor loop the corresponding loop current is zero as presented in Figure 7(b). This situation occurs when $i^r_n = i_e$.

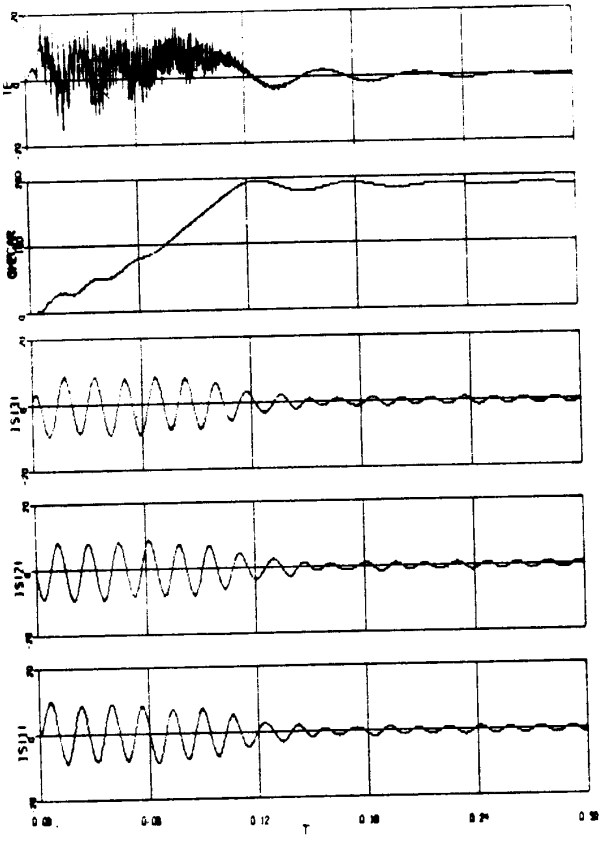

Figure 5 Stator currents in phases a, b and c; Speed; Torque (bottom to top). Balanced stator windings.

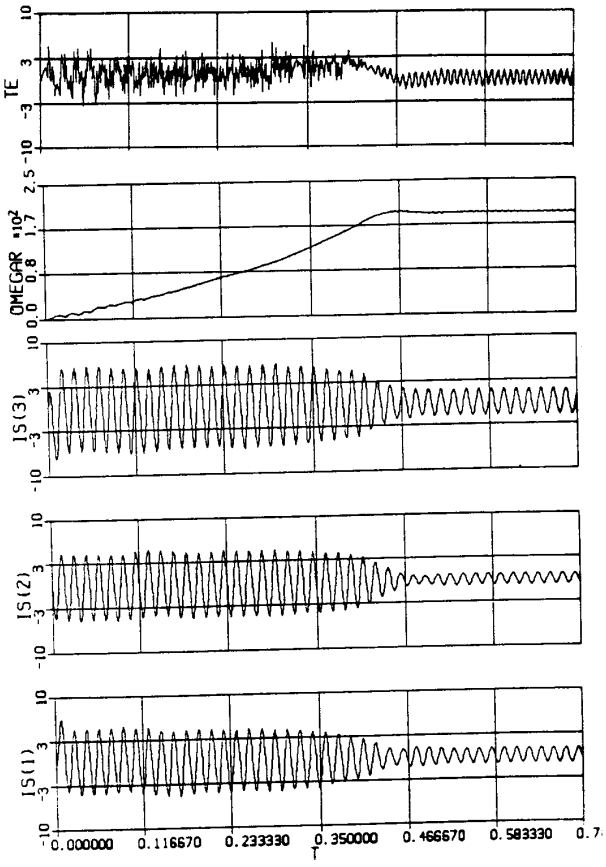

Figure 6 Stator currents in phases a, b and c; Speed; Torque (bottom to top). Stator windings asymmetry.

Figure 8 illustrates the electromagnetic torque, speed and the phase currents of the machine for the case of four broken rotor bars and one broken end ring, during a start up with a balanced sinusoidal voltage supply. It can be observed that the effect of four broken bars and single end ring on the machine phase currents in the transient and steady state is very noticeable.

It is important to note that the effects of space harmonics as simulated in this paper, typically result in torque pulsations. However, the winding functions are modeled with sharp edges thus the effect of space harmonics are accentuated. Therefore, the higher frequency components observed in Figures (5-7) would not be present in the real machine.

Figure 9(a) shows a frequency spectrum of the stator current at steady state for the loaded machine. Figure 9(b) represents the spectrum of the stator current when four bars and one endring segment are broken. A marked increase in the lower sideband of first harmonic (LSB1) which is (1-2s) times the synchronous frequency, 55.6 Hz at 1725 r/min, is obvious [7]. This harmonic can be used to detect the rotor failures as found by other authors [3,7,14].

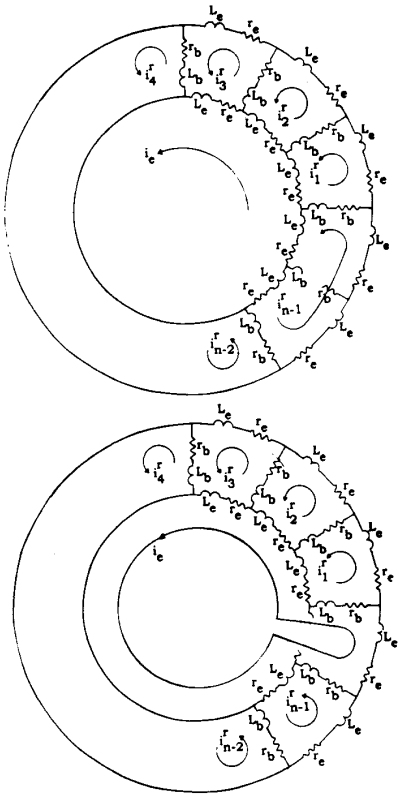

Figure 7 *a) Representation of broken bars. b) Representation of broken end rings.*

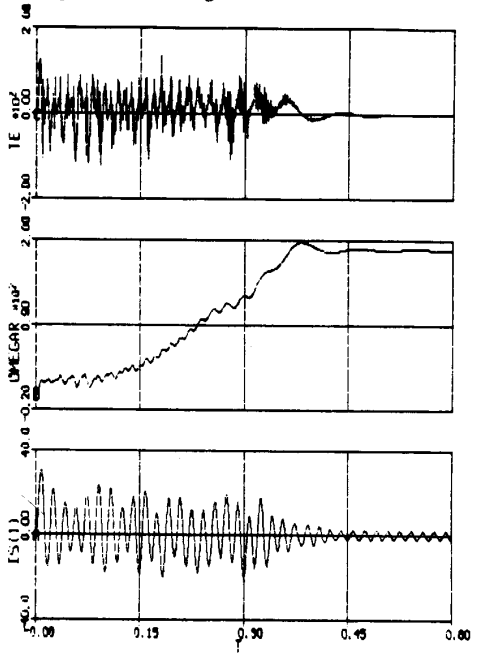

Figure 8 *Stator current; Speed; Torque (top to bottom). Rotor cage asymmetry.*

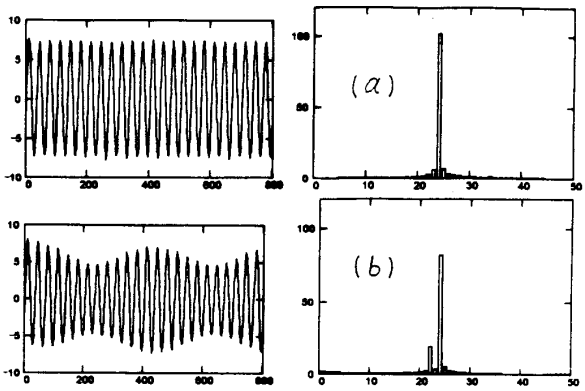

Figure 9 *Stator current spectra for a) Healthy motor, b) Four bars and one end ring broken.*

IV. Experimental Results

Figure 10 shows experimental transient phase currents for the 1hp, 60Hz, 4 pole, 208/460V induction machine with stator winding asymmetry due to shorting of one of the two coils of the phase c, for the case of balanced sinusoidal voltage supply. As predicted by the digital computer simulation results in Figure 6 for the same induction machine, the phase c current is higher than the phase a and b currents by approximately 40% compared to the symmetrically balanced case. It is clear that the experimental results are in close agreement with the dynamic simulation results given in Figure 6.

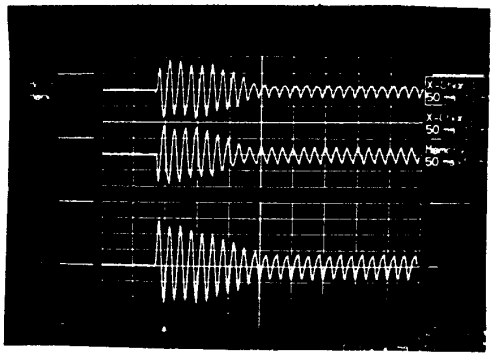

Figure 10 *Transient stator currents in phases a, b, and c (top to bottom). Scale: Current 1A/div, Time: 5 ms/div.*

V. CONCLUSIONS

The equations describing the performance of multi-phase induction machines during the transient as well as steady state behavior including the effects of stator asymmetry, broken rotor bars, and broken end rings have been derived in this paper. Space harmonics have been included in deriving these equations. Equations for calculation of electromagnetic torque have also been modified to account for non sinusoidal air gap flux distributions. To illustrate the utility of this method, two different induction machines with stator and rotor asymmetries with balanced

sinusoidal voltage supply have been simulated. Comparison of simulation and experimental results have verified the accuracy of the proposed method.

Acknowledgments

The authors wish to express their gratitude to Mr. William Dittman of Marathon Electric, Wausau, Wisconsin, for the assistance provided.

Appendix

Machine Parameters

1 HP, 460/230V, 4-pole	7.5HP, 460V, 4-pole, 3phase
ℓ =47.752 mm	ℓ =102.4128 mm
g = .3175 mm	g = .456438 mm
r = 47.14875 mm	r = 63.2968 mm
N = 82	N = 90
R_s = 17.88 Ω	R_s = 3.5332 Ω
L_s = .025 H	L_s = .028 H
r_b = 52.86E-6 Ω	r_b = 68.34E-6 Ω
L_b = .12E-6 H	L_b = .28E-6 H
r_e = 2.01E-6 Ω	r_e = 1.56E-6 Ω
L_e = .03E-6 H	L_e = .03E-6 H

References

[1] H. Weichel, "Squirrel Cage Rotors with Split Resistance Rings," Journal AIEE, 1928, 47, pp. 929-943.

[2] E. Mishkin, "Disturbances in the Induction Machine due to Broken Squirrel Cage Rings," Journal Franklin Institute, 259, pp. 133-143., 1955.

[3] S. Williamson, and A.C. Smith, "Steady State Analysis of 3 Phase Cage Motors with Rotor Bar and End Ring Faults," Proc. IEE , vol. 129, pt. B, No. 3, pp. 93-100, May 1982.

[4] P. Vas, "Investigation of Squirrel Cage Induction Motors with Concentrated Rotor Asymmetries," Electrotechnika, vol. 68, pp. 461-463, 1975.

[5] P. Vas, "Steady State Operation of Squirrel Cage Induction Motors with General Asymmetry," JEEE, (India), vol. 59, pt. EL6, pp. 303-308, 1979.

[6] P.C. Krause, C.H. Thomas, "Simulation of Symmetrical Induction Machinery", AIEE Transactions on Power Apparatus and Systems, vol. PAS-84, No. 11, Nov. 1965, pp.1038-1053.

[7] G.B. Kliman, R.A. Koegl, J. Stein, R.D. Endicott, and M.W. Madden, "Noninvasive Detection of Broken Rotor Bars in Operating Induction Motors," IEEE Transaction on Energy Conversion, vol. 3, No. 4, pp. 873-879, Dec. 1988.

[8] H.A. Toliyat, M.M. Rahimian, S. Bhattacharya, and T.A. Lipo, "Transient Analysis of Induction Machines Under Internal Faults Using Winding Functions," Third International Conference on Electrical Rotating Machines-ELROMA '92, Bombay, India.

[9] T.A. Lipo, and H.A. Toliyat, "Feasibility Study of a Converter Optimized Induction Motor," Palo Alto, California; Electric Power Research Institute, January 1989, EPRI Final Report 2624-02.

[10] H.A. Toliyat, T.A. Lipo, and J.C. White, "Analysis of a Concentrated Winding Induction Machine for Adjustable Speed Drive Applications- part I (Motor Analysis)," IEEE Transactions on Energy Conversion, vol. 6, No. 4, pp. 679-684, Dec. 1991.

[11] H.A. Toliyat, T.A. Lipo, and J.C. White, "Analysis of a Concentrated Winding Induction Machine for Adjustable Speed Drive Applications- part II (Motor Design and Performance)," IEEE Transactions on Energy Conversion, vol. 6, No. 4, pp. 685-692, Dec. 1991.

[12] H.A. Toliyat, L.Y. Xue, and T.A. Lipo, "A Five Phase Reluctance Motor with High Specific Torque," IEEE Transactions on Industry Applications, vol. 28, No. 3, pp. 659-667, May/June 1992.

[13] C.F. Landy, W. Levy, and M.D. McCulloch, "The Effect of Broken Rotor Bars on the Torque Speed Curve of Squirrel Cage Induction Motors," Proc. of International Conference on Electrical Machines (ICEM '90), Boston, USA, pp. 510-515.

[14] N.M. Elkasabgy, A.R. Eastham, and G.E. Dawson, "Detection of Broken Bars in the Cage Rotor on an Induction Machine,"IEEE Transactions on Industry Applications, vol. 28, No. 1, pp. 165-171, Jan./Feb. 1992.

Hamid A. Toliyat (S'87-M'91) was born in Mashhad, Iran, in 1957. He received the B.S. (1982) and M.S. (1986) in electrical engineering from Sharif University of Technology, Tehran, Iran and West Virginia University, Morgantown, W.V. respectively. Between 1982 and 1984 he worked for power companies in Iran. He received his Ph.D. degree in electrical engineering from the University of Wisconsin-Madison in 1991. In 1991 he joined the faculty of Ferdowsi University-Mashhad, Mashhad, Iran, and is now an Assistant Professor of Electrical Engineering.

Dr. Toliyat is a member of the IEEE Power Engineering Society and Sigma Xi. His main research areas include converter optimized induction and synchronous reluctance machines, power electronics, power systems and control.

Thomas A. Lipo (F'87) is a native of Milwaukee, Wisconsin. He received his B.E.E. and M.S.E.E. degrees from Marquette University, Milwaukee, WI in 1962 and 1964 and the Ph.D. degree in Electrical Engineering from the University of Wisconsin in 1968. From 1969 to 1979 he was an Electrical Engineer in the Power Electronics Laboratory of Corporate Research and Development of the General Electric Company, Schenectady, NY.

He became Professor of Electrical Engineering at Purdue University in 1979 and in 1981 he joined the University of Wisconsin in the same capacity. Dr. Lipo has maintained a deep research interest in power electronics and ac drives for over 25 years. He has received twelve IEEE prize paper awards for his work including co-recipient of the Best Paper Award in the IEEE Industry Applications Society Transactions for the year 1984. In 1986 he received the Outstanding Achievement Award from the IEEE Industry Applications Society for his contributions to the field of ac drives and in 1990 he received the William E. Newell Award of the IEEE Power Electronics Society for his contributions to power electronics.